Graphical Abstract

To create your abstract, type over the instructions in the template box below.
Fonts or abstract dimensions should not be changed or altered.

Type the title of your article here

Authors' names here

Departmental address here

Leave this area blank for abstract info.

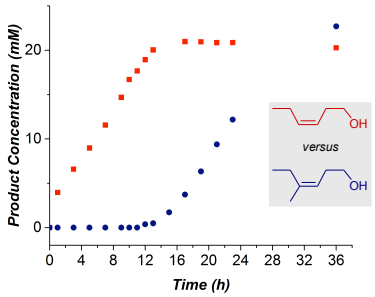

Tetrahedron
journal homepage: www.elsevier.com

Relative reactivity of alkenyl alcohols in the Palladium-catalyzed redox-relay Heck reaction

Margaret J. Hilton[a] , Bin Cheng[a] , Benjamin R. Buckley[a], Liping Xu[b], Olaf Wiest[b,c] and Matthew S. Sigman[a]*

[a]*Department of Chemistry, University of Utah, 315 S. 1400 East, Salt Lake City, UT 84112*
[b]*Lab of Computational Chemistry and Drug Design, Laboratory of Chemical Genomics, Peking University Shenzhen Graduate School, Shenzhen 518055, China*
[c]*Department of Chemistry and Biochemistry, University of Notre Dame, Notre Dame, Indiana 46556-5670, United States*

ARTICLE INFO

Article history:
Received
Received in revised form
Accepted
Available online

Keywords:
redox-relay;
Heck reaction;
relative rates of alkenes;
competition experiments

ABSTRACT

The relative rates of alkenyl alcohols in the Pd-catalyzed redox-relay Heck reaction were measured in order to examine the effect of their steric and electronic properties on the rate-determining step. Competition experiments between an allylic alkenyl alcohol and two substrates with differing chain lengths revealed that the allylic alcohol reacts about three times faster in both cases. Competition between a di- and trisubstituted alkenyl alcohols provided an interesting scenario, in which the disubstituted alkene was consumed first followed by consumption of the trisubstituted alkene. Consistent with this observation, the transition state structures for the migratory insertion of the aryl group into the di- and trisubstituted alkenes were calculated with a reduced barrier for the disubstituted alkene. An internal competition between a substrate containing two alcohols with differing chain lengths demonstrated the catalyst's preference for migrating towards the closest alcohol. Additionally, it was observed that increasing the electron density in the arene boronic acid promotes a faster reaction, which correlates with Hammett σ_p values where ρ= -0.87.

* Corresponding author. e-mail: sigman@chem.utah.edu

1. Introduction

In recent years, we have reported a redox-relay strategy[1-3] in the context of a Heck reaction[4] with alkenyl alcohols, wherein an enantioselective arylation occurs and the alkene unsaturation is relayed to the chain-terminating alcohol (Figure 1).[5-7] Both tertiary[5,6] and quaternary centers[7] may be established in high enantioselectivity while a new functional group, a ketone or aldehyde, is concomitantly formed during the process at various distances from the original alkene.

Due to this reactions robust ability to impart high enantioselectivity and its interesting trends in site selectivity, it has been the focus of a number of mechanistic studies,[8-10] which support a rate-determining arylation step followed by successive β-hydride elimination and migratory insertion steps until the carbonyl product is released (Figure 1). Computational analysis[9,10] of the reaction coordinate reveals a relatively flat energy surface after the initial migratory insertion of the aryl group, which is the site and enantioselectivity-determining step. Enantioselectivity is controlled by repulsion between the *t*Bu group on the oxazoline *Ligand* and the alkenol and by a stabilizing C–H π interaction between the aryl group and the pyridyl ring. The electronic and steric nature of the arene and the alkene do not have a notable effect on enantioselectivity yet

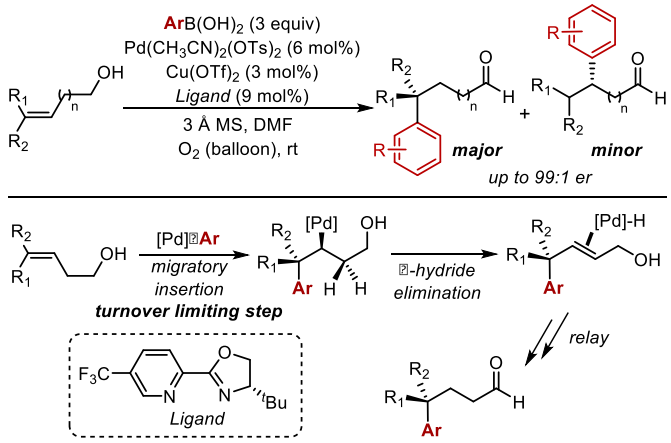

Figure 1. Enantioselective redox-relay Heck arylation

significantly affect the site selection, as was described using Hammett σ values[6], IR vibrations[11], and NBO charges.[9] We hypothesize that polarization during the migratory insertion transition state, leading to subtle electronic differences in the alkene carbons, controls the site selectivity. Consequently, site selectivity increases with decreasing electron-density in the arene, increasing steric bulk on the alkene, and decreasing chain length in the alkenol. Examination of these factors on the rate of the reaction would provide further insight for future catalyst design and substrate compatibility, improving reaction rates, carrying out cascade reactions, and selectively functionalizing complex starting materials.

2. Results and Discussion

Herein, we report kinetic data to delineate the effect on reaction rate of substituents on the boronic acid and of the chain length between the alcohol and alkene on the substrate. The kinetics were measured by observing the formation of the products by gas chromatography. In general, we observed overall zero order kinetics through multiple half lives. This suggests that transmetallation of the boronic acid is fast prior to rapid alkene binding, leading to a saturated catalyst, which undergoes a rate limiting migratory insertion. This is consistent with the computational results. To further probe this hypothesis, several electronically differentiated boronic acid derivatives were evaluated under the same reaction conditions. The rate of product formation is dependent on the nature of the boronic acid, which is consistent with rate limiting migratory insertion. More nucleophilic electron-rich arenes react faster than their electron-poor counterparts, which correlates with Hammett σ_p values with a $\rho = -0.87$ (Figure 2).

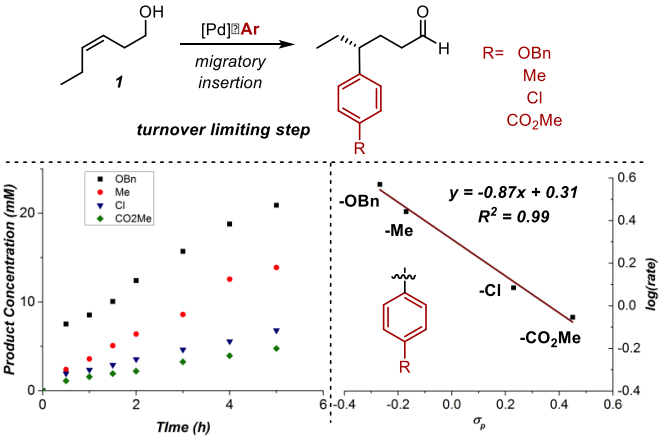

Figure 2. Effect of arene electronic nature on reaction rate

An interesting feature of this reaction is that similar enantioselectivity but different site selectivity is observed as a function of the distance between the alkene and the alcohol. A question arising from these results pertains to the relative reactivity of the different alkenes. Understanding the potential differences may allow for strategic reaction design wherein two unique alkenes undergo selective reactions. Therefore, the effect of chain length on the reaction rate was examined through competition experiments. As allylic and homoallylic alcohols have been the main focus of the previous reports in terms of both scope and computational analysis, we initially evaluated the relative rate of **1** and **2** (Figure 3a). In the experiment, the allylic alcohol reacts 4.4 times faster than the homoallylic alcohol. Of note, independent rate measurements of **1** show that the overall rate is retarded by ~5 times in the presence of **2** (Figure S1). These results suggest that reversible binding of the alkene occurs and that the allylic alcohol reacts faster in a Curtin-Hammett controlled reaction. To further explore this, the competitive rates between **2** and **3**, a trishomoallylic alcohol, were measured (Figure 3b). Again, the allylic alkenol reacted faster (3.6 times) than the substrate with a longer chain. Nearly identical competitive rates were observed for **1** and **3**, which suggests that the homoallylic and trishomoallylic alcohol have similar reactivity in this reaction. To test this, a competitive reaction of the two (**1** and **3**) was performed. Similar reactivity of the two alkenes was measured, wherein the relative rates are almost identical (Figure 3c).

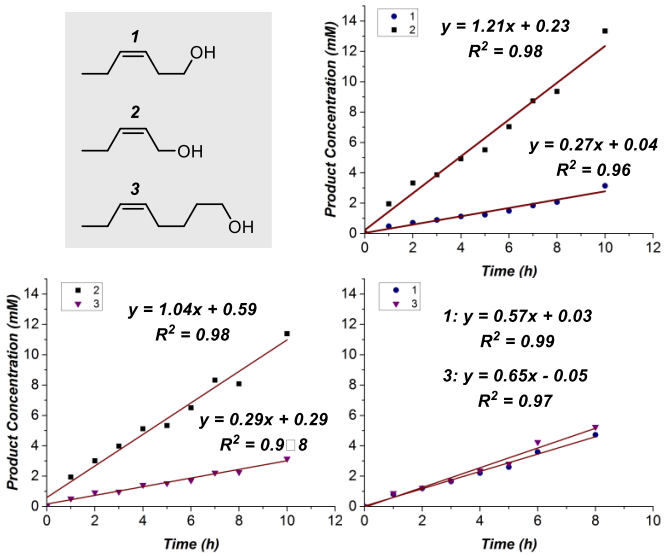

Figure 3. Effect of chain length on rate. Competition experiments between a) homoallylic **1** and allylic **2**, b) trishomoallylic **3** and allylic **2**, and c) homoallylic **1** and trishomoallylic **3** alkenols.

A surprising aspect of these results is the enhanced reactivity of the allylic alcohol, since the computed barrier for migratory insertion of the aryl group into a homoallylic alkenol has a lower activation energy of 0.5 kcal/mol.[10] However, the complexity of the outersphere of the metal coordination environment may not be accounted for in the computations, wherein hydrogen bonding, counterion effects and solvent organization likely impact the reaction. Therefore, a possible explanation is a lower contribution to entropy-driven preorganization of the allylic substrate and the catalyst promotes a faster reaction, compared to substrates with longer chains.[12]

As this reaction operates on both di- and trisubstituted alkenols, we were interested in determining their relative rates. Empirically, trisubstituted alkenols were found to take more time to be consumed. However, trisubstituted alkenes are more electron rich and, thus, determining the relative rates would delineate whether the empirical results were a function of a steric effect. Consistent with our previous observations, the homoallylic disubstituted alkene **1** reacts significantly faster than the homoallylic trisubstituted alkene **4** (Figure 4). An interesting feature of this competitive scenario is that **1** is consumed before any reaction of the trisubstituted alkene. In other words, there was no simultaneous reaction of **1** and **4**. However, the rate of consumption of the homoallylic alcohol is slightly inhibited, again suggesting the reaction is under Curtin-Hammett control.

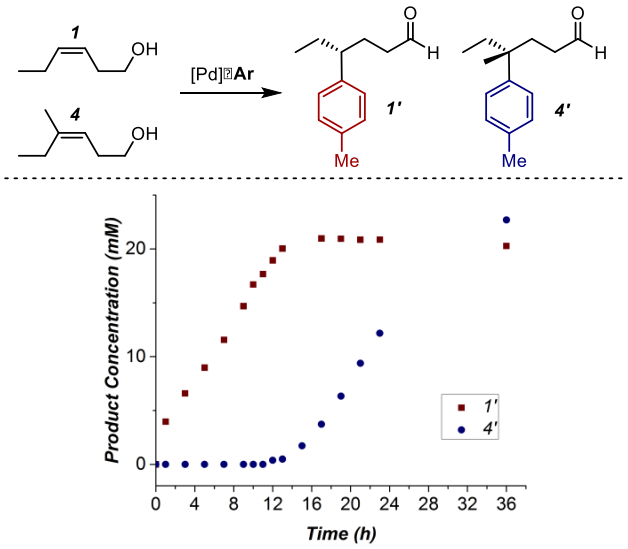

Figure 4. Competition between di- and trisubstituted alkenes

To further investigate the origin of this observation, we calculated the relevant transition structures. We reported previously[8,9] that the selectivity determining and turnover limiting step is the migratory insertion through **TS1** (Figure 5a). We have now computed the analogous transition structure **TS2** for the trisubstituted olefin (Figure 5a). The $\Delta\Delta G^{\neq}$ is 1.1 kcal/mol in preference for the disubstituted alkene, which is in agreement with the experimentally measured relative rates. For the disubstituted alkene, the closest H–H bond distances are relatively long (2.22 and 2.30Å), and the dihedral angle for the insertion step is 8.8°. In comparison, the distances become shorter (2.20 and 2.13 Å) for the trisubstituted alkene (**TS2**), inducing more steric repulsion and a greater distorted dihedral angle (16.2°). This is in agreement with the main rate controlling factor being steric in nature.

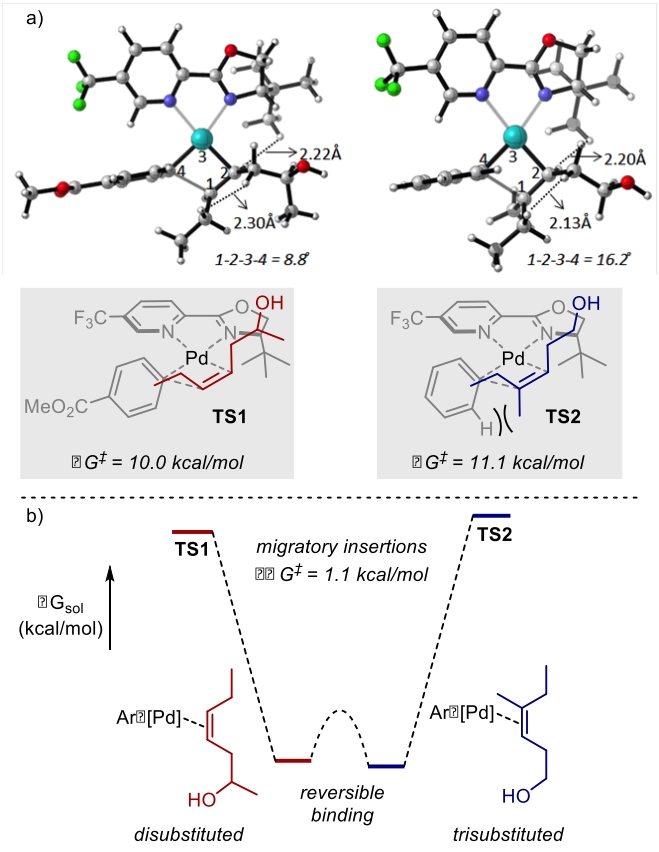

Figure 5. a) Computed transition states for migratory insertion of the aryl group. b) Curtin-Hammett control

Finally, we wished to interrogate the relative selectivity during the relay process in terms of how the catalyst determines which hydrogen undergoes β-hydride elimination. As this process is post rate limiting, we designed two substrates which contain a branch point with two different distances to the attached alcohols. After initial migratory insertion, this internal competition presumably proceeds through relay to the branch point, wherein the catalyst must select to chain-walk towards either alcohol from intermediate **A** (Figure 6). Our recent isotopic labeling studies suggest that chain-walking is likely to be unidirectional towards the alcohol.[8] In the event, the product distribution of the resulting aldehydes from **5** (6.5:1) and **6** (___) reveals that the catalyst prefers to relay towards the closer alcohol. This is consistent with our previous computational analysis and isotopic labeling experiments, which reveal lower energetic Pd-intermediates as the catalyst migrates towards the alcohol. Thus, it is energetically favorable for the catalyst to prefer the shorter distance between the branching point and the alcohol in substrates **5** and **6**.

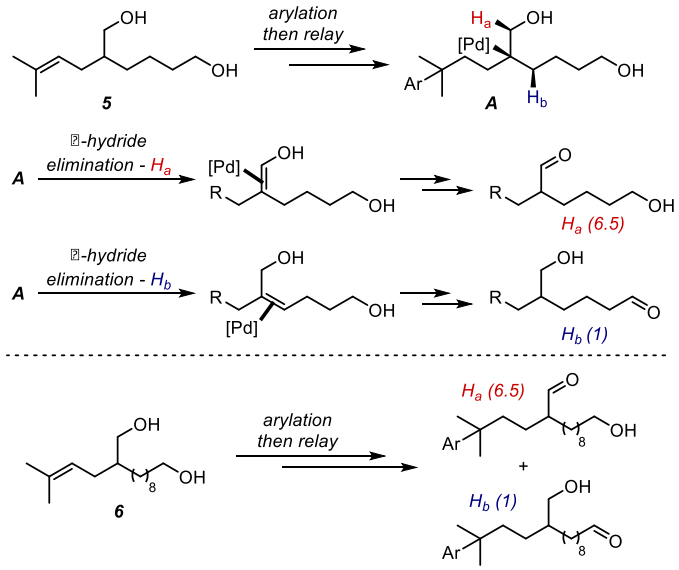

Figure 6. Internal competition between alcohols of differing chain lengths

3. Conclusions

The relative reactivity of various alkenes in the redox-relay Heck reaction has provided valuable insight into the subtle effects on the migratory insertion step. The distance between the alkene and the alcohol does not significantly affect the rate of reaction, except in the case of allylic alcohols. Studies are ongoing to understand this observation. In addition, di- and trisubstituted alkenes are non-competitive in the rate limiting step, although competitive alkene binding is observed. Of practical note, this result indicates that selective functionalization of disubstituted alkenes in the presences of trisubstituted alkenes could be a viable option for late stage introduction in complex molecules. Moreover, selective carbonyl formation from the redox-relay process is also possible, with preference for the alcohol that lies closer to the site of alkene addition.

4. Experimental section

General Methods

Dry dimethylformamide (DMF) was stored over activated 3 Å molecular sieves. $Pd(CH_3CN)_2(OTs)_2$ and *Ligand* were synthesized according to literature procedures.[5,13] All starting materials were commercially available, and were used without further purification. All products except **1'** and **X** have been previously characterized.,[6,7] Spectra of the products from this study were in agreement with the previously characterized materials.[6,7] ^{1}H-NMR spectra were obtained at 500 MHz; chemical shifts are reported in ppm, and referenced to the $CHCl_3$ singlet at 7.26 ppm. ^{13}C-NMR spectra were obtained at 125 MHz and referenced to the center peak of the $CDCl_3$ signals at 77.0 ppm. The abbreviations s, d, t, q, and m stand for the resonance multiplicities singlet, doublet, triplet, and multiplet, respectively. Analysis by gas chromatography (GC) was performed using a Hewlett Packard HP 6890 series GC system fitted with an Agilent HP-5 column. Each kinetic experiment was carried out in a 10 mL round bottom flask equipped with a side arm and was repeated twice. Rates were determined by GC measurements of products (both regioisomers) relative to an internal standard of 2-methoxynapthalene.

Computational Methods

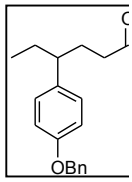

All calculations were performed using M06[14] functional implemented in Gaussian09.[15] The Lanl2DZ and 6-31+G(d) basis sets were used for Pd and all other atoms, respectively. Single point calculations using the SDD basis set for Pd and the 6-311++G(d, p) basis set for all other atoms and the SMD solvent model with the parameters for DMF were used to account for solvent effects. Frequency calculations at the same level of theory at the optimized geometries were carried out to conform the stationary points as minima (no imaginary frequency) or transition state (one imaginary frequency) and provided the thermal corrections to the single point energies.

Competition Experiments

Standard solutions of $Pd(CH_3CN)_2(OTs)_2$, $Cu(OTf)_2$, *Ligand*, and alkene were prepared in DMF for each set of experiments. The appropriate amounts were added to individual reactions to give 0.05 M concentration with equimolar amounts of competing alkene (totaling 0.3 mmol), palladium catalyst (6 mol%), copper co-catalyst (3 mol%), and *Ligand* (9 mol%). The solutions containing palladium, copper, and ligand were mixed, and then the alkene was added. Boronic acid (3 equiv) and powdered molecular sieves (45 mg, 150 mg/mmol) were added to the reaction flask, which was subsequently purged with O_2. Once the reaction mixture was added to the reaction flask, aliquots (~100 µL) were removed periodically and passed through a silica plug eluting with ethyl acetate for GC analysis.

Effect of Boronic Acid

The same general procedure as described for the competition experiments was followed using *cis*-5-hexen-1-ol. Conditions were maintained in each experiment, yet the substitution (R) at the *para*-position of the boronic acid was changed, according to the Hammett series below.

R	Hammett σ_p	Rate (mM/h)
OBn	-0.27	3.71
Me	-0.17	2.77
Cl	+0.23	1.22
CO_2Me	+0.45	0.88

Note: plots of product formation over time can be found in the supplementary material (Figure S1)

4-(p-Tolyl)hexanal (**1'**)

cis-5-Hexen-1-ol (20.0 mg, 0.2 mmol) was dissolved in DMF (2 ml) and in a separate vial Ligand (4.9 mg, 9 mol%), $Pd(CH_3CN)_2(OTs)_2$ (6.4 mg, 6 mol%), and $Cu(OTf)_2$ (2.1 mg, 3 mol%) were also dissolved in DMF (2 mL). Powdered molecular sieves (25 mg) and 4-methylphenyl boronic acid (81.6 mg, 3 equiv) were added to a 10 mL round bottom flask, which was subsequently purged with oxygen. The solutions were mixed and added to the reaction flask. The reaction was allowed to stir for 18 hours at room temperature and was quenched by addition of brine and diluted with diethyl ether. The aqueous layer was extracted with diethyl ether (2 x 10 mL), and the combined organic layers were washed with brine (2 x 10 mL). The organic layer was dried over magnesium sulfate, and the solvent was evaporated *in vacuo*. The crude product, was purified by flash chromatography (1-5% EtOAc/Hexanes) to afford the aldehyde **1'** (17.0 mg, 45%, colorless oil) as mixture of regioisomers (3.7:1). R_f (20% EtOAc/Hexanes) 0.74; FT-IR (neat) 2923.8, 1722.1, 1513.9, 1456.6, 815.9, 668.2, 548.7 cm^{-1}; ^{1}H-NMR (500 MHz, $CDC1_3$) 9.65 (1H, t, *J* 1.5 Hz), 7.11 (2H, d, *J* 8.0 Hz), 7.00 (2H, d, *J* 8.0 Hz), 2.41-2.35 (1H, m), 2.32 (3H, s), 2.30-2.24 (2H, m), 2.04-1.98 (1H, m), 1.83-1.76 (1H, m), 1.72-1.64 (1H, m), 1.62-1.56 (1H, m), 0.78 (3H, t, *J* 7.5 Hz) ppm; $^{13}C\{^1H\}$-NMR (125 MHz, $CDCl_3$) 202.8, 141.4, 136.0, 129.4, 127.8, 47.0, 39.1, 30.0, 28.8, 20.7, 12.4 ppm; HRMS (TOF ES+): MNa^+, found 213.1249. $C_{13}H_{18}ONa$ requires 213.1255.

4-(4-(Benzyloxy)phenyl)hexanal (**X**)

Prepared in an identical manner to **1'** described above employing 4-benzyloxyphenyl boronic acid (xx mg, xx mmol), afforded the aldehyde **X** (32.1 mg, 57%, white semi-solid) as a mixture of regioisomers (3.2:1). R_f (20% EtOAc/Hexanes) 0.58; FT-IR (neat) 2930.7, 2022.7, 1723.3, 1652.9, 1558.7, 1455.8, 836.5, 750.0, 667.9 cm^{-1}; ^{1}H-NMR (500 MHz, $CDC1_3$) 9.66 (1H, t, *J* 1.5 Hz), 7.44 (2H, d, *J* 7.5 Hz), 7.39 (2H, t, *J* 7.5 Hz), 7.33 (1H, t, *J* 8.0 Hz), 7.04 (2H, d, *J* 9.0 Hz), 6.93 (2H, d, *J* 9.0 Hz), 5.04 (2H, s), *2*.41-2.35 (1H, m), 2.33-2.22 (2H, m), 2.04-1.98 (1H, m), 1.82-1.75 (1H, m), 1.72-1.64 (1H, m), 1.62-1.52 (1H, m), 0.79 (3H, t, *J* 7.5 Hz) ppm; $^{13}C\{^1H\}$-NMR (125 MHz, $CDCl_3$) 202.8, 157.6, 137.4, 136.8, 128.8, 128.6, 128.2, 127.8, 115.1, 70.3, 46.6, 42.5, 30.0, 29.0, 12.4 ppm; HRMS (TOF ES+): MNa^+, found 305.1522. $C_{19}H_{22}O_2Na$ requires 305.1517.

Acknowledgments

BRB would like to thank Loughborough University for study leave funding.

Supplementary Material

Kinetic plots not presented herein, NMR spectra, details of the computational results… can be found in the supplementary material.

5. References

(1) Burns, N. Z.; Baran, P. S.; Hoffmann, R. W. *Angewandte Chemie International Edition* **2009**, *48*, 2854.

(2) Renata, H.; Zhou, Q.; Baran, P. S. *Science* **2013**, *339*, 59.

(3) Weinstein, A. B.; Schuman, D. P.; Tan, Z. X.; Stahl, S. S. *Angewandte Chemie International Edition* **2013**, *52*, 11867.

(4) Heck, R. F. *Journal of the American Chemical Society* **1968**, *90*, 5518.

(5) Werner, E. W.; Mei, T.-S.; Burckle, A. J.; Sigman, M. S. *Science* **2012**, *338*, 1455.

(6) Mei, T.-S.; Werner, E. W.; Burckle, A. J.; Sigman, M. S. *Journal of the American Chemical Society* **2013**, *135*, 6830.

(7) Mei, T.-S.; Patel, H. H.; Sigman, M. S. *Nature* **2014**, *508*, 340.

(8) Hilton, M. J.; Xu, L.-P.; Norrby, P.-O.; Wu, Y.-D.; Wiest, O.; Sigman, M. S. *The Journal of Organic Chemistry* **2014**.

(9) Xu, L.; Hilton, M. J.; Zhang, X.; Norrby, P.-O.; Wu, Y.-D.; Sigman, M. S.; Wiest, O. *Journal of the American Chemical Society* **2014**, *136*, 1960.

(10) Dang, Y.; Qu, S.; Wang, Z.-X.; Wang, X. *Journal of the American Chemical Society* **2013**, *136*, 986.

(11) Milo, A.; Bess, E. N.; Sigman, M. S. *Nature* **2014**, *507*, 210.

(12) Kang, S. O.; Lynch, V. M.; Day, V. W.; Anslyn, E. V. *Organometallics* **2011**, *30*, 6233.

(13) Drent, E. v. B., J. A. M.; Doyle, M. J. *J. Organomet. Chem.* **1991**, *417*, 235.

(14) Zhao, Y.; Truhlar, D. *Theor Chem Account* **2008**, *120*, 215.

(15) Frisch, M. J. e. a. *Gaussion09* **2009**.

**Frisch, M. J. et al. *Gaussion09*; Gaussian: Wallingford, CT, 2009.